Published in final edited form as:
Cancer Res. 2012 December 15; 72(24): 6457–6467. doi:10.1158/0008-5472.CAN-12-1340.

Modulation of the ATPase and transport activities of broad-acting multidrug resistance factor ABCC10 (MRP7)

Ekaterina V. Malofeeva[1], **Natalya Domanitskaya**[1], **Mariya Gudima**[1], and **Elizabeth A. Hopper-Borge**[1,*]

[1]Program in Developmental Therapeutics, Fox Chase Cancer Center, Philadelphia, 19111

Abstract

The cell surface molecule ABCC10 is a broad-acting transporter of xenobiotics, including cancer drugs such as taxanes, epothilone B, and modulators of the estrogen pathway. *Abcc10*$^{-/-}$ mice exhibit increased tissue sensitivity and lethality resulting from paclitaxel exposure compared to wild-type counterparts, arguing ABCC10 functions as a major determinant of taxane sensitivity in mice. To better understand the mechanistic basis of ABCC10 action, we characterized the biochemical and vectorial transport properties of this protein. Using crude membranes in an ABCC10 overexpression system, we found that the ABCC10 transport substrates $E_2$17βG and LTC_4 significantly stimulated ABCC10 BeFX-sensitive ATPase activity. We also defined the $E_2$17βG antagonist, tamoxifen, as a novel substrate and stimulator of ABCC10. In addition, a number of cytotoxic substrates, including docetaxel, paclitaxel and Ara-C, increased the ABCC10 basal ATPase activity. We determined that ABCC10 localizes to the basolateral cell surface, using transepithelial well assays to establish that ABCC10-overexpressing LLC-PK1 cells exported [^{3}H]-docetaxel from the apical to the basolateral side. Importantly, we found that the clinically valuable multi-kinase inhibitor sorafenib, and a natural alkaloid, cepharanthine, inhibited ABCC10 docetaxel transport activity. Thus, concomitant use of these agents might restore the intracellular accumulation and potency of ABCC10-exported cytotoxic drugs such as paclitaxel. Overall, our work could seed future efforts to identify inhibitors and other physiological substrates of ABCC10.

Keywords

ATPase activity; transport; basolateral; ABCC10; docetaxel; cepharanthine; sorafenib

Introduction

The phenomenon of multidrug resistance (MDR) remains a substantial problem in the chemotherapeutic treatment of cancer. One important contributing factor in MDR is the overexpression of a class of efflux pumps known as ATP-Binding Cassette (ABC) transporters. The C sub-family of ATP binding cassette proteins is alternatively known as the ABCC proteins, or the Multidrug Resistance Protein (MRP) subfamily. Members of this subfamily confer resistance to and transport several classes of chemotherapeutics including taxanes, vinca alkaloids, camptothecans, and nucleoside analogs, as well as physiological substrates including leukotrienes and glutathione (1, 2). This ABCC group consists of 9 family members conserving a common structural organization that includes at least two transmembrane domains (TMDs) and nucleotide-binding domains (NBDs) (2). The ABCC

*To whom correspondence should be addressed: Elizabeth Hopper-Borge, Fox Chase Cancer Center, 333 Cottman Avenue, Philadelphia, PA. 19111, Phone: 215-214-1505, Fax: 215-728-3616, EA_Hopper@fccc.edu.

sub-family is further divided into two groups: ABCC1 (MRP1), ABCC2 (MRP2), ABCC3 (MRP3), ABCC6 (MRP6) and ABCC10 (MRP7) have additional N-terminal transmembrane domains, while ABCC4 (MRP4), ABCC5 (MRP5), ABCC11 (MRP8), and ABCC12 (MRP9) do not (2).

ABCC10 consists of three TMDs and two NBDs, and is one of the least well characterized family members (3), although we and others have demonstrated that ABCC10 tissue expression is widespread (4). Recent work has suggested that ABCC10 expression level is elevated in non small cell lung cancer (NSCLC) in relation to normal lung, with ABCC10 expression in adenocarcinoma correlated with tumor grade and stage (5). Supporting a potential role for ABCC10 in control of the response of tumors to the administration of therapeutics, we have previously shown that overexpression of ABCC10 *in vitro* confers resistance to an unusually wide range of clinically valuable drugs, including taxanes, vinca alkaloids, nucleoside analogs and epothilone B (6–8). Excitingly, we have recently used a newly developed Abcc10$^{-/-}$ mouse model to show that absence of this transporter *in vivo* sensitizes animals to taxanes, with Abcc10$^{-/-}$ mice experiencing increased sensitivity (i.e., neutropenia, and bone marrow hypoplasia) compared to their wild-type counterparts following paclitaxel treatment.

Together, these findings suggest that modulation of ABCC10 activity by inhibitors may have clinical value in management of human cancers such as NSCLC. Currently ATPase activities have been described for some of the longer ABCC subfamily members, including ABCC1, ABCC2, ABCC3 and ABCC6 (9–12) and also for ABCC4 (13). However, to date, neither the enzymatic activity of the ABCC10 ATPase nor the mechanistic basis for ABCC10 transport of substrates have been substantially investigated. This study addresses these points, by characterizing the effects of modulators on biochemical and transport properties of ABCC10.

Materials and methods

Cell lines

LLC-PK1 cells were purchased from the American Type Culture Collection (ATCC), (Manassas, VA) 7 years ago. All ATCC cell lines undergo authentication tests during the accessioning process using methods described in the online ATCC brochure *Maintaining High Standards in Cell Culture*. These characterizations are applied to the final seed and distribution stocks of cell lines for certification include testing viability of the cell population just prior to freezing and immediately after thawing by trypan-blue dye-exclusion test. Observations of recovery and growth are recorded along with morphological appearance. The ATCC also uses isoenzymology and/or the Cytochrome C subunit I (COI) PCR assay is performed for species confirmation. Cells were passaged in our laboratory for fewer than 3 months after receipt or resuscitation. The High Five cell line was purchased three years ago from Invitrogen (Carlsbad, CA). Cells were passaged in our laboratory for fewer than 3 months after receipt or resuscitation. These cells have not been authenticated.

Reagents

Trizma hydrochloride, D-mannitol, ethylene glycol tetraacetic acid, dithiothreitol, ammonium molybdate, antimony potassium tartarate, sulfuric acid, potassium chloride, ouabain powder, magnesium chloride, L-ascorbic acid, sodium dodecyl sulfate, sodium azide, beryllium sulfate tetrahydrate, sodium fluoride, sodium orthovanadate (Vi), cobalt (II) chloride, calcium chloride, manganese (II) chloride, protease inhibitors, bovine serum albumin, glycerol, N-methyl-D-glucamine, adenosine triphosphate (ATP), adenosine diphosphate (ADP), lucifer yellow CH dipotassium salt, tamoxifen, 17β-estradiol-D-17β-

glucuronide, glutathione (GSH), leukotriene C4 (LTC_4), docetaxel, paclitaxel, cytosine β-D-arabinofuranoside (Ara-C), cisplatinum and epothilone B (EpoB) were purchased from Sigma-Aldrich (St. Louis, MO, USA). [^{3}H]-docetaxel (5 Ci/mmol) was obtained from Moravek Biochemicals Inc. (Brea, California, USA).

Preparation of ABCC10-transfected LLC-PK1 cells

ABCC10 expression vector and parental plasmid were transfected into LLC-PKI cells using Lipofectamine (according to the manufacturer's instructions, Invitrogen, Carlsbad, CA). Individual colonies were selected in medium containing gentamicin (1000 μg/ml) and expanded for further analysis. Two clones in which ABCC10 protein was detected by immunoblot analysis were employed in the present study. The cells are routinely tested (every 3 to 6 months) for mycoplasma contamination and for ABCC10 protein expression. LLC-ABCC10 and empty vector-transfected control cells were cultured in medium 199 supplemented with 10% fetal bovine serum, 50 units/ml penicillin, 50 μg/ml streptomycin, 2 mM L-glutamine, 800 μg/ml gentamicin. All cell lines were grown at 37°C with 5% CO_2 under humidifying conditions.

Expression and identification of ABCC10 and ABCC1 in High Five Insect Cells

High Five insect cells (Invitrogen, Carlsbad, CA, USA) were infected with the recombinant baculovirus containing the ABCC1 or ABCC10 cDNA. To create the recombinant baculovirus, ABCC1 and ABCC10 cDNA were cloned into pFastBac CT-TOPO vector (Invitrogen, Carlsbad, CA, USA). Crude membranes were prepared as previously described (14) and used in subsequent ATPase assays. Total protein was estimated using an Amido Black protein-filter assay of Schaffner and Weissmann with bovine serum albumin as a standard. The membrane fraction was then resuspended to a concentration of 1 mg/ml and stored at −80°C until use. Crude membranes were electrophoresed on a 3–8% NuPAGE gel (Invitrogen) and stained with Colloidal blue (Invitrogen) following the manufacturer's instructions. Following electrotransfer to nitrocellulose paper, blots were probed with the previously described ABCC10 monoclonal antibody at a dilution of 1:10 (7) or the previously described Abcc10 polyclonal antibody (15) at a dilution of 1:3000 and an anti ABCC1 mouse monoclonal QCRL-1 (Santa Cruz Biotechnology, Inc, CA, USA) at a dilution of 1:100.

Preparation of membranes

Total cell membranes were prepared from LLC-PK1 cells by Dounce homogenization in PM-buffer (1M HEPES, 1M $MgCl_2$1M KCl) containing protease inhibitors: 5 μg/ml aprotinin, 5 μg/ml leupeptin, 2 μg/ml pepstatin, 100 mM PMSF (phenylmethyl sulfonyl fluoride). Intact cells and nuclei were removed by centrifugation at 500 g for 10 min at 4°C, and then the supernatant spun at 3000g for 10 min at 4°C. Cell membranes were pelleted by centrifugation at 10000 g for 45 min at 4°C and resuspended in PM-buffer.

For immunoblot analysis, 10–40 μg of membrane proteins was analyzed on a 8% SDS-PAGE gel and transferred to nitrocellulose filters using a wet transfer system, as described previously (16). The blots were incubated with the previously described ABCC10 monoclonal antibody at a dilution of 1:10 (7) or the previously described Abcc10 polyclonal antibody (15). After washing, the blots were incubated with horseradish peroxidase secondary goat anti-rabbit IgG (NEN, Boston, MA). β-actin-HRP (Abcam, Cambridge, MA) conjugated antibody was used at a dilution of 1:5000.

Beryllium Fluoride-induced [α-^{32}P]-8-azidoADP trapping in ABCC10

BeFx-induced [α- ^{32}P]-8-azidoADP trapping assays contained ATPase assay buffer, 0.5 mM BeFx, 20 mM $MgCl_2$, 1 mg/ml of membrane ABCC10, and 100 μM [α-^{32}P]-8-azidoATP (2.5–10 uCi/nmol) ("Affinity Photoprobes, LLC"). Reactions were preincubated in low light in the absence of [α-^{32}P]-8-azidoATP at 37°C for 3 min, initiated by the addition of [α-^{32}P]-8-azidoATP and quenched by adding ice-cold ATP (100 mM). Reactions were irradiated by UV light (365 nm wavelength) on ice for 10 min and subjected to SDS-PAGE and after drying, the gel was exposed to film for 12–72 hours.

Measurement of ATPase activity

ATPase activity was measured by the endpoint Pi assay as previously described (17). ABCC10 and ABCC1 specific activity was recorded as vanadate or BeFx-sensitive ATPase activity. The amount of inorganic phosphate released over 20 min at 37°C was measured. 2X ATPase assay buffer (100 mM Tris-HCl pH 7.5, 1M KCl, 0.25M sodium azide, 0.125 M EGTA, 1 mM ouabain, 1M DTT) was combined with 2M $MgCl_2$, 5–10 μg of membrane protein, and various drugs or substrates for a 5 min preincubation at 37°C. The reaction was initiated by 5 mM ATP addition and quenched with 100 μl of 5% SDS. The amount of Pi released was quantitated using a previously described colorimetric method (13). Kinetic parameters were determined by linear regression analysis of the Lineweaver-Burk transformation of the data by using GraphPad Prism 4 software. Velocity = $V = V_{max}$ [S]/([S] + K_m), where:V_{max} is the limiting velocity as substrate concentrations get very large. [S] is concentration of substrate; K_m is the concentration of substrate that leads to half-maximal velocity (in Molar). All data were statistically analyzed with a Student's unpaired *t*-test and *P*-values less than 0.05 were considered statistically significant.

Drug accumulation

For drug accumulation, control LLC-pcDNA 3.1 cells, ABCC10-transfected LLC-ABCC10-11 and LLC-ABCC10-16 cells were seeded in duplicate at a density of 2×10^5 cells per well in 6-well plate. The next day the media was replaced with media containing 0.1 μM [^{3}H]-docetaxel (5 Ci/mmol, Movarek, Brea, CA) to a final concentration and cells were incubated at 37°C. For inhibition studies the cells were preincubated with the modulators cepharanthine (5 μM) or tyrosine kinase inhibitors as indicated in the results (2.5 μM) for 1 hour. After preincubation, the solution was removed and labeled substrate with modulators was added to the well for 15, 30 and 60 min incubation at 37°C. After incubation, cells were washed with ice-cold PBS and trypsinized. An aliquot of cells was used to determine cell number, and the remaining cells were then washed three times with ice-cold PBS. Each sample was placed in scintillation fluid to measure the radioactivity in a liquid scintillation counter. All data were statistically analyzed with a Student's unpaired *t*-test and *P*-values less than 0.05 was considered statistically significant.

Transepithelial transport

Cells were seeded on microporous polycarbonate membrane filters (3.0 μm pore size, 6.5 mm insert, Transwell 3415, Costar) at a density of 1×10^6 cells per well for LLC-PK1 cells in 24-well plates. The cells were grown for 7 days in complete medium, with medium replacement after day one and then every two days until the day of the experiment. Once the transepithelial electrical resistance (TEER) reached >500 Ωcm^2 and when Lucifer yellow rejection reached 97–100% (18, 19), the experiment was started by adding HBSS containing 0.1 μM [^{3}H]-docetaxel (5 Ci/mmol) to either the apical or basolateral side. For the inhibition study, after washing steps, the cells were preincubated with modulators for 1 hour. After incubation the solutions were aspirated and labeled substrate was added to the donor chamber, while refilling fresh modulator solution in both chambers. The cells were

incubated at 37°C in 5% $CO_2$and 25 μl aliquots were taken from the receiver side at 0, 2, 6, 12, 20 and 30 min, and placed in scintillation fluid to measure the radioactivity in liquid scintillation counter. The apparent permeability coefficient (P_{app}) was calculated as previously described (19). All data were statistically analyzed with a Student's unpaired *t*-test and *P*-values less than 0.05 was considered statistically significant.

Confocal laser scanning microscopy

LLC-PK ABCC10 transfectants were grown on cover slips for ~3 days until cells reached confluency. After PBS washing, fixation, solubilization, and blocking, cells were incubated with rabbit polyclonal C-terminus-ABCC10 antibody (diluted 1:50 in blocking buffer) (15) and mouse anti-β-catenin (dilution 1:500) (BD Transduction Laboratories, San Diego, CA, USA) for 1 hour at room temperature. Secondary antibody included anti-rabbit conjugated to Alexa-488 and anti-mouse conjugated to Alexa-568. DAPI (4', 6-diamidino-2-phenylindole) (Molecular Probes/Invitrogen, Carlsbad, CA) was used to stain DNA at a dilution of 1:2000. The cells were mounted on a glass slide with ProLonged Antifade Reagent (Molecular probes). Confocal laser scanning microscopy was performed with a Nikon C1 spectral confocal microscope (Nikon, Melville, NY, USA).

Results

Expression and identification of human ABCC10 and ABCC1 in Hi-Five insect cells

To support study of ABCC10 ATPase activity, ABCC10 and ABCC1 (a well characterized transporter used as a positive control) (20, 21) were overexpressed using a baculovirus system. ABCC10 and ABCC1 were readily detected in crude membrane fractions as full length proteins, with almost no truncation or degradation byproducts (Figures 1A, 1B). Purified ABCC10 bound effectively to the nucleotide analog [α-^{32}P]-8-azidoATP, confirming structural integrity of the nucleotide binding domains (NBDs) (13) (Figure 1C).

Basal properties of ABCC10-mediated ATP hydrolysis

ABCC10 ATPase activity was measured using an inorganic phosphate (Pi) release assay (17), with ouabain, EGTA, and sodium azide added to crude membrane preparations to eliminate confounding Na^+/K^+Ca^{2+} and mitochondrial ATPase activity, as in (22). Under these conditions, the basal rate of ATP hydrolysis of ABCC10 ranged from 5.5–12 nmole/min/mg protein (Figure 2A and data not shown), depending on the preparation. For reference, ABCC1 activity was 5–10 nmole/min/mg protein using purified and reconstituted protein (9), and approximately 4–5 nmol/min/mg protein in our system (data not shown). The non-covalent ATPase inhibitors orthovanadate (Vi) and beryllium fluoride (BeFx) replace phosphate during ATP hydrolysis, and stabilize a specific, transition state conformation, inhibiting ATPase activity; prior work has shown individual ABC transporters respond differently to these inhibitors, reflecting differences in catalytic activity (13, 23, 24). We determined that ABCC10 ATPase activity is more sensitive to BeFx than Vi (32% and 11.4% inhibition, respectively) (Figure 2A-B). For ABCC1, the BeFx-dependent inhibition was almost 2 fold more effective than Vi inhibition (60% versus 35%, respectively), in accord with previously reported values (25) (Figure 2A-B).

Environmental pH can significantly affect transporter ATPase activity (19, 22, 26–28). Optimal ABCC10 ATPase activity occurred at pH 7.5 (Figure 2C), comparable to that reported for ABCC1 (9). Titration of ATP revealed maximal ABCC10 activity at a concentration of approximately 6 mM (Figure 2D). We analyzed the kinetics over a concentration range from 0–8 mM ATP using a Lineweaver–Burk analysis. We determined that the ABCC10 K_m value for ATP binding is 3.2 mM, in contrast to a 0.1 mM K_m value of ABCC1 (25). ABCC10 ATPase activity was inhibited at [ATP] > 9 mM. Prior work on

other ATPases have observed similar inhibitory effects under conditions where other factors required for catalysis, such as [Mg^{2+}], are present in limiting concentrations (29). Discrete ATPases typically have varying requirements for divalent cations during ATP hydrolysis (13, 30). As anticipated, ABCC10-mediated ATP hydrolysis is cation dependent; we established a rank order preference of Mn^{2+}>Mg^{2+}>Ca^{2+}>Co^{2+} (Figure 2E), with Mn^{2+} increasing ATPase activity by 52% compared with Mg^{2+}.

Dose-dependent induction of ABCC10 ATPase activity by physiological substrates and anti-cancer agents

Leukotriene C4 (LTC_4), the estrogen estradiol-glucuronide ($E_2$17βG) and glutathione (GSH) are physiological substrates for ABCC1, and induce ABCC1 ATPase activity (31, 32). We tested these compounds for activation of ABCC10, using the crude membrane system described above. We found that LTC_4 and $E_2$17βG induced ABCC10 ATPase activity by 79.7% and 30%, respectively (Figure 3A, 3C). Maximal induction of ABCC10 ATPase activity was observed for LTC_4 at 1 μM. Further analyses of the effect of LTC_4 on ABCC10 ATPase activity revealed that at concentrations under 1 μM, the K_m=0.057 μM for LTC_4 (Figure 3C inset). The compound tamoxifen is frequently used in breast cancer treatments as an estrogen receptor antagonist, based on competition with estradiol. Interestingly, we found that tamoxifen is also a modest substrate for ABCC10, and at lower tamoxifen concentrations (less than 2 μM) the K_m=0.078 μM (Figure 3B inset). However, at higher concentrations LTC_4 and tamoxifen both inhibited ABCC10 ATPase activity. In contrast, GSH had no significant effect on ABCC10 ATPase activity at ~1 μM, a concentration stimulatory for ABCC1 (Figure 3D). As controls, we confirmed that leukotriene C4 and glutathione are ATPase-inducing substrates for ABCC1 (Figure 3E, 3F) (9, 20, 21). Taken together, these data indicate that while LTC_4 and $E_2$17βG interact similarly with the ABCC1 and ABCC10 ATPase domains, GSH does not stimulate ABCC10 ATPase activity. We observed that at high concentrations all substrates inhibited ABCC1 and ABCC10 ATPase activity as previously described for ABCB1 (33). It has been previously described that ABC transporter substrates can be categorized into three distinct types: 1. agents that stimulate ATPase activity at low concentration, but inhibit activity at high concentration; 2. agents that enhance ATPase activity in a dose-dependent manner; and 3. agents that inhibit ATPase activity (as for ABCB1) (34). Therefore, the ABCC10 substrates $LTC_4$and $E_2$17βG are classified into the first group and GSH falls into the third class of agents.

We have shown that the growth of ABCC10-transfected HEK293 cells is resistant to taxanes, *vinca* alkaloids, the non-taxane anti-microtubule agent epothilone, and the nucleoside analog Ara-C, but not to cisplatin (7, 35). We assessed the drug-stimulatable ATPase activity of ABCC10 using two drug concentrations (0.625 μM and 5 μM) of the taxanes (docetaxel and paclitaxel), Ara-C, epothilone B, and cisplatin. We used vector transfected pFastBac membranes as a control, and ABCB1-overexpressing membranes for comparison (Figure 4A-C). A maximal 31.8% stimulation in activity of ABCC10 was induced by Ara-C at a concentration of 0.625 μM and (Figure 4A). At 5 μM, paclitaxel, and docetaxel stimulated ABCC10 ATPase activity by 15% and 24.38%, respectively (Figure 4B), while in contrast, these compounds stimulated ABCB1 ATPase activity by 63% and 36%, respectively. However, the basal ATPase activity for ABCB1 was reduced 3-fold in comparison to ABCC10 activity. (Figure 4C). Surprisingly, epothilone B did not affect ABCC10 ATPase activity, even though overexpressed ABCC10 causes resistance to this compound (7). As expected, the negative control cisplatin, a non-substrate (6), did not influence the ATPase activity ATPase activity of ABCC10 or ABCC1.

Localization and docetaxel transport properties of ABCC10 in polarized LLC-PK1 cells

ABC transporters variously localize to the apical or basolateral cell surface, affecting their transport properties (36, 37). To study the localization and transport properties of ABCC10, we overexpressed ABCC10 in a polarized pig kidney epithelial cell line, LLC-PK1 (Figure 5A). ABCC10 localized predominantly to the basolateral membranes in two independent ABCC10-overexpressing LLC-PK1 derivative cell lines (Figure 5B).

As anticipated, these ABCC10-overexpressing cell lines exhibited reduced accumulation of [^{3}H]-docetaxel compared with parental vector-transfected LLC-pcDNA3.1 cells (51% and 63%, respectively, at 60 min time point) (Figure 6A). A transepithelial well assay was used to assess transport of [^{3}H]-docetaxel initially added to either the apical or the basolateral side of a cell monolayer. Polarized LLC-PK1 ABCC10-overexpressing cells line predominantly exported [^{3}H]-docetaxel from the apical to the basolateral side (Figure 6B). While the parental cell line revealed no differences between apical-to-basolateral or basolateral-to-apical docetaxel transport, in contrast, we found that apical to basolateral transport of ABCC10-overexpressing derivative cell lines were 70–80% higher than for LLC-PK1 parental apical-to-basolateral transport. This data correlated with the localization of ABCC10 (Figure 5); ABCC10's basolateral localization indicated that ABCC10-dependent transport should be directional from the apical to basolateral side.

Cepharanthine and tyrosine kinase inhibitors (TKIs) modulate ABCC10 ATPase activity, accumulation, and transcellular transport of [^{3}H]-docetaxel

The natural product cepharanthine has previously been established as a modulator of ABCC10-dependent resistance and transport activity (38). Clinically valuable TKIs such as imatinib, lapatinib, erlotinib and nilotinib have also been shown to inhibit ABCC10 *in vitro* (39–41). We determined that at 5 μM, cepharanthine, sorafenib, imatinib, nilotinib, erlotinib and lapatinib were effective inhibitors of ABCC10 ATPase activity. At 0.625 μM, nilotinib and erlotinib potently inhibited ABCC10 ATPase activity by 41.4% and 47%, respectively (Figure 7A). Finally, dasatinib had no effect on ATPase activity of ABCC10 at any concentration tested.

Treatment of ABCC10-overexpressing cells (LLC-ABCC10-11 and LLC-ABCC10-16) with 5 μM cepharanthine significantly increased accumulation of [^{3}H]-docetaxel (by 48.4% and 22.5%, at 60 min, respectively), compared to accumulation levels without inhibitor. In contrast, 2.5μM sorafenib increased [^{3}H]-docetaxel accumulation by 22.4% in LLCABCC10-16 cells and by 49% in LLC-ABCC10-11 cells, compared to accumulation levels without inhibitor (Figure 7B). 2.5μM dasatinib also increased [^{3}H]-docetaxel intracellular accumulation without significant effects on ABCC10 ATPase activity. Conversely, 2.5μM lapatinib (a reported ABCC10 reversal agent (40) did not affect the accumulation levels of docetaxel, but decreased ABCC10 ATPase activity. Other TKIs with reported activity in inhibiting ABCC10 such as nilotinib and erlotinib, only affected [^{3}H]-docetaxel accumulation of the LLC-ABCC10-11 cell line, while imatinib only inhibited the LLC-ABCC10-16 cell line (Figure 7B). Interestingly, nilotinib, dasatinib, imatinib and lapatinib significantly decreased [^{3}H]-docetaxel accumulation of the parental LLC-pcDNA3.1 cell line, indicating additional activities not targeted at ABCC10.

Since our data revealed that [^{3}H]-docetaxel accumulation was significantly inhibited by sorafenib in both transfectants, we tested if sorafenib could also inhibit ABCC10 transepithelial transport using cepharanthine as a positive control. We showed that cepharanthine was the most potent inhibitor of ABCC10 mediated [^{3}H]-docetaxel accumulation in both transfectants (Figure 7B). Finally, we also established that transepithelial apical to basolateral transport of labeled docetaxel was inhibited by 5μM

cepharanthine in LLC-ABCC10-16 (Figure 7C). 2.5μM sorafenib maximally inhibited apical to basolateral transport for the LLC-ABCC10-16 cell line at 6–30 minutes (Figure 7C).

Discussion

To date, the localization, biochemical and transport properties of ABCC10 have been largely unexplored, with the exception of a single study that used a membrane vesicle transport system (42). In the present study, the biochemical properties of ABCC10 were compared to the well described properties of ABCC1, the first identified ABCC subfamily member (20). Despite significant sequence identity (50.3/52.7%) within the two nucleotide binding domains and appreciable overall amino acid identity (33.8%) between ABCC10 and ABCC1 (6), ABCC10 transports taxanes and confers *in vivo* taxane resistance, and does not require glutathione for transport, in contrast to ABCC1 (6). Our characterization of ABCC10 basal activity revealed that ABCC10 was far less sensitive to vanadate (11%) or BeFX (32%) inhibition than ABCC1 (35% and 60%, respectively), or the other major taxane pump, ABCB1, which has been reported to be completely inhibited (43). Taken together, these data imply that the catalytic cycle of ABCC10 differs from the well-described cycles of ABCC1 and ABCB1. As anticipated, we found that ABCC10 ATPase activity is stimulated by its substrates, the taxanes and Ara-C, similar to the best described taxane pump, ABCB1 (44). Surprisingly, however, the extremely weak ABCC10 transport substrate LTC_4stimulated ABCC10 activity significantly more than ABCC1 activity (~80% versus ~30%), even though LTC_4 is a well established physiological substrate for ABCC1. This unexpected result further highlights differences between these proteins, and emphasizes the need for further study (9, 45).

Knowledge of intracellular distribution is important for understanding the potential effects of ABCC10-mediated transport in normal tissues, and to provide insight with respect to putative substrates. In the present study, we demonstrated that ABCC10 localizes basolaterally when ectopically expressed in the LLC-PK1 kidney cell line, similar to the localization reported for ABCC1 in small intestine and kidney cells. In contrast, ABCB1 localizes apically in brain, liver, small intestine and kidney (46, 47). ABCC10 transcript expression is widespread, with highest levels detected in the gonads and spleen (7). The ABCC10 transcript has been detected in multiple types of adenocarcinoma that are routinely treated with taxanes, including breast, ovary and lung (4, 48, 49). Recent studies have shown that ABCC10 is also upregulated in hepatocellular carcinoma compared with normal adjacent healthy liver samples (50) and that ABCC10 gene levels in colorectal tumors correlate with tumor grade ($P = 0.01$) (51), implying that increased ABCC10 expression might be a biomarker for and regulator of treatment response in certain cancers. However, aside from a single study examining ABCC10 protein expression in lung cancer (5), no studies have been published regarding ABCC10 protein expression. It will be of considerable interest to assess ABCC10 protein expression levels in tumors versus normal tissues in the context of treatment with taxanes.

Our recent work has indicated that loss of Abcc10 function *in vivo* causes taxane sensitization (15). In this report, we have shown that cepharanthine and sorafenib (an agent used to treat unresectable and advanced hepatocellular carcinoma) were effective inhibitors of ABCC10 ATPase activity. Likewise, we showed that cepharanthine increased docetaxel accumulation in ABCC10-overexpressing cells and inhibited apical to basolateral transport, particularly at early timepoints (at 6–12 minutes). Interestingly, we found that sorafenib promoted increased [H^3]-docetaxel accumulation in two LLC-ABCC10 transfectants. The identification of sorafenib as an ABCC10 inhibitor suggests that *in vivo* action of this inhibitor may involve modulation of ABCC10-dependent docetaxel transport. Currently, no identified inhibitors have been shown to have *in vivo* efficacy against ABCC10; an

important goal for future work would be the exploration of the ability of sorafenib, cepharanthine, and other putative inhibitors to modulate *in vivo* taxane transport capabilities of ABCC10 in preclinical models. ABCC10 inhibition is particularly nominated as a potentially high value target for inhibition based on its physiological relevance to *in vivo* taxane resistance. The loss of no other single transporter (including ABCB1) has resulted in tissue sensitization to taxanes, suggesting no other transporter can be upregulated to compensate for Abcc10 loss (15). Whether absence of ABCC10 sensitizes solid tumors to taxanes while not leading to unacceptable toxicity in normal tissue remains to be determined. These investigations are currently ongoing in our laboratory.

In summary, this study provided the first analysis of ABCC10 ATPase activity, showed that ABCC10 localized basolaterally in a polarized kidney cell line, and confirmed this localization by demonstrating apical to basolateral transport. Importantly, we also identified a novel inhibitor of ABCC10 transport. These ABCC10 assays can be used to identify and validate potential ABCC10 modulators that can be validated in preclinical models with the goal to increase the clinical effectiveness of ABCC10 drug substrates.

Supplementary Material

Refer to Web version on PubMed Central for supplementary material.

Acknowledgments

We are particularly grateful to Dr. Suresh Ambudkar (NCI) for his guidance, advice and help in preparation of the initial ABCC10 virus used in this project. We thank Dr. Susan Cole for the MRP1 cDNA. We also thank Drs. Jonathan Chernoff and Jeffrey R. Peterson (Fox Chase Cancer Center, Philadelphia, PA) for helpful discussions and review of the manuscript. We also acknowledge Dr. Erica A. Golemis (Fox Chase Cancer Center) for critical reading and review of the manuscript. We also thank Karen Trush for assistance with preparation of the figures.

Grant support

This work was supported by National Institutes of Health grants K01CA120091 to E.H.B, and CA06927 to Fox Chase Cancer Center.

References

1. Keppler D. Multidrug resistance proteins (MRPs, ABCCs): importance for pathophysiology and drug therapy. Handb Exp Pharmacol. 2011; 201:299–323. [PubMed: 21103974]
2. Glavinas H, Krajcsi P, Cserepes J, Sarkadi B. The role of ABC transporters in drug resistance, metabolism and toxicity. Curr Drug Deliv. 2004 Jan; 1(1):27–42. [PubMed: 16305368]
3. Kruh GD, Guo Y, Hopper-Borge E, Belinsky MG, Chen ZS. ABCC10, ABCC11, and ABCC12. Pflugers Arch. 2007 Feb; 453(5):675–684. [PubMed: 16868766]
4. Takayanagi S, Kataoka T, Ohara O, Oishi M, Kuo MT, Ishikawa T. Human ATP-binding cassette transporter ABCC10: expression profile and p53-dependent upregulation. J Exp Ther Oncol. 2004 Oct; 4(3):239–246. [PubMed: 15724843]
5. Wang P, Zhang Z, Gao K, Deng Y, Zhao J, Liu B, et al. [Expression and Clinical Significance of ABCC10 in the Patients with Non-small Cell Lung Cancer.]. Zhongguo Fei Ai Za Zhi. 2009 Aug 20; 12(8):875–878. [PubMed: 20719174]
6. Hopper-Borge E, Chen ZS, Shchaveleva I, Belinsky MG, Kruh GD. Analysis of the drug resistance profile of multidrug resistance protein 7 (ABCC10): resistance to docetaxel. Cancer Res. 2004 Jul 15; 64(14):4927–4930. [PubMed: 15256465]
7. Hopper-Borge E, Xu X, Shen T, Shi Z, Chen ZS, Kruh GD. Human multidrug resistance protein 7 (ABCC10) is a resistance factor for nucleoside analogues and epothilone B. Cancer Res. 2009 Jan 1; 69(1):178–184. [PubMed: 19118001]

8. Oguri T, Ozasa H, Uemura T, Bessho Y, Miyazaki M, Maeno K, et al. MRP7/ABCC10 expression is a predictive biomarker for the resistance to paclitaxel in non-small cell lung cancer. Mol Cancer Ther. 2008 May; 7(5):1150–1155. [PubMed: 18445659]

9. Mao Q, Leslie EM, Deeley RG, Cole SP. ATPase activity of purified and reconstituted multidrug resistance protein MRP1 from drug-selected H69AR cells. Biochim Biophys Acta. 1999 Nov 9; 1461(1):69–82. [PubMed: 10556489]

10. Hagmann W, Nies AT, Konig J, Frey M, Zentgraf H, Keppler D. Purification of the human apical conjugate export pump MRP2 reconstitution and functional characterization as substrate-stimulated ATPase. Eur J Biochem. 1999 Oct 1; 265(1):281–289. [PubMed: 10491184]

11. Chloupkova M, Pickert A, Lee JY, Souza S, Trinh YT, Connelly SM, et al. Expression of 25 human ABC transporters in the yeast Pichia pastoris and characterization of the purified ABCC3 ATPase activity. Biochemistry. 2007 Jul 10; 46(27):7992–8003. [PubMed: 17569508]

12. Cai J, Daoud R, Alqawi O, Georges E, Pelletier J, Gros P. Nucleotide binding and nucleotide hydrolysis properties of the ABC transporter MRP6 (ABCC6). Biochemistry. 2002 Jun 25; 41(25): 8058–8067. [PubMed: 12069597]

13. Sauna ZE, Nandigama K, Ambudkar SV. Multidrug resistance protein 4 (ABCC4)-mediated ATP hydrolysis: effect of transport substrates and characterization of the post-hydrolysis transition state. J Biol Chem. 2004 Nov 19; 279(47):48855–48864. [PubMed: 15364914]

14. Sauna ZE, Smith MM, Muller M, Kerr KM, Ambudkar SV. The mechanism of action of multidrug-resistance-linked P-glycoprotein. J Bioenerg Biomembr. 2001 Dec; 33(6):481–491. [PubMed: 11804190]

15. Hopper-Borge EA, Churchill T, Paulose C, Nicolas E, Jacobs JD, Ngo O, et al. Contribution of Abcc10 (Mrp7) to in vivo paclitaxel resistance as assessed in Abcc10(−/−) mice. Cancer Res. 2011 May 15; 71(10):3649–3657. [PubMed: 21576088]

16. Towbin H, Staehelin T, Gordon J. Electrophoretic transfer of proteins from polyacrylamide gels to nitrocellulose sheets: procedure and some applications. 1979. Biotechnology. 1992; 24:145–149. [PubMed: 1422008]

17. DeGorter MK, Conseil G, Deeley RG, Campbell RL, Cole SP. Molecular modeling of the human multidrug resistance protein 1 (MRP1/ABCC1). Biochem Biophys Res Commun. 2008 Jan 4; 365(1):29–34. [PubMed: 17980150]

18. Irvine JD, Takahashi L, Lockhart K, Cheong J, Tolan JW, Selick HE, et al. MDCK (Madin-Darby canine kidney) cells: A tool for membrane permeability screening. J Pharm Sci. 1999 Jan; 88(1): 28–33. [PubMed: 9874698]

19. Spears KJ, Ross J, Stenhouse A, Ward CJ, Goh LB, Wolf CR, et al. Directional trans-epithelial transport of organic anions in porcine LLC-PK1 cells that co-express human OATP1B1 (OATP-C) and MRP2. Biochem Pharmacol. 2005 Feb 1; 69(3):415–423. [PubMed: 15652233]

20. Deeley RG, Cole SP. Substrate recognition and transport by multidrug resistance protein 1 (ABCC1). FEBS Lett. 2006 Feb 13; 580(4):1103–1111. [PubMed: 16387301]

21. Cole SP, Deeley RG. Transport of glutathione and glutathione conjugates by MRP1. Trends Pharmacol Sci. 2006 Aug; 27(8):438–446. [PubMed: 16820223]

22. Lanzetta PA, Alvarez LJ, Reinach PS, Candia OA. An improved assay for nanomole amounts of inorganic phosphate. Anal Biochem. 1979 Nov 15; 100(1):95–97. [PubMed: 161695]

23. Sankaran B, Bhagat S, Senior AE. Inhibition of P-glycoprotein ATPase activity by beryllium fluoride. Biochemistry. 1997 Jun 3; 36(22):6847–6853. [PubMed: 9184168]

24. Rao US. Drug binding and nucleotide hydrolyzability are essential requirements in the vanadate-induced inhibition of the human P-glycoprotein ATPase. Biochemistry. 1998 Oct 20; 37(42): 14981–14988. [PubMed: 9778376]

25. Hipfner DR, Deeley RG, Cole SP. Structural, mechanistic and clinical aspects of MRP1. Biochim Biophys Acta. 1999 Dec 6; 1461(2):359–376. [PubMed: 10581367]

26. Kerr KM, Sauna ZE, Ambudkar SV. Correlation between steady-state ATP hydrolysis and vanadate-induced ADP trapping in Human P-glycoprotein. Evidence for ADP release as the rate-limiting step in the catalytic cycle and its modulation by substrates. J Biol Chem. 2001 Mar 23; 276(12):8657–8664. [PubMed: 11121420]

27. Marchetti S, Oostendorp RL, Pluim D, van Eijndhoven M, van Tellingen O, Schinkel AH, et al. In vitro transport of gimatecan (7-t-butoxyiminomethylcamptothecin) by breast cancer resistance protein, P-glycoprotein, and multidrug resistance protein 2. Mol Cancer Ther. 2007 Dec; 6(12 Pt 1):3307–3313. [PubMed: 18089724]

28. Shibayama Y, Nakano K, Maeda H, Taguchi M, Ikeda R, Sugawara M, et al. Multidrug resistance protein 2 implicates anticancer drug-resistance to sorafenib. Biol Pharm Bull. 2011 Mar; 34(3): 433–435. [PubMed: 21372398]

29. Syroeshkin AV, Galkin MA, Sedlov AV, Vinogradov AD. Kinetic mechanism of Fo x F1 mitochondrial ATPase: Mg2+ requirement for Mg x ATP hydrolysis. Biochemistry (Mosc). 1999 Oct; 64(10):1128–1137. [PubMed: 10561559]

30. Kerr ID. Structure and association of ATP-binding cassette transporter nucleotide-binding domains. Biochim Biophys Acta. 2002 Mar 19; 1561(1):47–64. [PubMed: 11988180]

31. Hooijberg JH, Pinedo HM, Vrasdonk C, Priebe W, Lankelma J, Broxterman HJ. The effect of glutathione on the ATPase activity of MRP1 in its natural membranes. FEBS Lett. 2000 Mar 3; 469(1):47–51. [PubMed: 10708754]

32. Mao Q, Deeley RG, Cole SP. Functional reconstitution of substrate transport by purified multidrug resistance protein MRP1 (ABCC1) in phospholipid vesicles. J Biol Chem. 2000 Nov 3; 275(44): 34166–34172. [PubMed: 10942765]

33. Najar IA, Sachin BS, Sharma SC, Satti NK, Suri KA, Johri RK. Modulation of P-glycoprotein ATPase activity by some phytoconstituents. Phytother Res. 2010 Mar; 24(3):454–458. [PubMed: 19653312]

34. Zhao XQ, Xie JD, Chen XG, Sim HM, Zhang X, Liang YJ, et al. Neratinib Reverses ATP-Binding Cassette B1-Mediated Chemotherapeutic Drug Resistance In Vitro, In Vivo, and Ex Vivo. Mol Pharmacol. 2012 Jul; 82(1):47–58. [PubMed: 22491935]

35. Hopper E, Belinsky MG, Zeng H, Tosolini A, Testa JR, Kruh GD. Analysis of the structure and expression pattern of MRP7 (ABCC10), a new member of the MRP subfamily. Cancer Lett. 2001 Jan 26; 162(2):181–191. [PubMed: 11146224]

36. Evers R, Zaman GJ, van Deemter L, Jansen H, Calafat J, Oomen LC, et al. Basolateral localization and export activity of the human multidrug resistance-associated protein in polarized pig kidney cells. J Clin Invest. 1996 Mar 1; 97(5):1211–1218. [PubMed: 8636432]

37. Deeley RG, Westlake C, Cole SP. Transmembrane transport of endo- and xenobiotics by mammalian ATP-binding cassette multidrug resistance proteins. Physiol Rev. 2006 Jul; 86(3): 849–899. [PubMed: 16816140]

38. Zhou Y, Hopper-Borge E, Shen T, Huang XC, Shi Z, Kuang YH, et al. Cepharanthine is a potent reversal agent for MRP7(ABCC10)-mediated multidrug resistance. Biochem Pharmacol. 2009 Mar 15; 77(6):993–1001. [PubMed: 19150344]

39. Hoffmann K, Franz C, Xiao Z, Mohr E, Serba S, Buchler MW, et al. Sorafenib modulates the gene expression of multi-drug resistance mediating ATP-binding cassette proteins in experimental hepatocellular carcinoma. Anticancer Res. 2010 Nov; 30(11):4503–4508. [PubMed: 21115899]

40. Kuang YH, Shen T, Chen X, Sodani K, Hopper-Borge E, Tiwari AK, et al. Lapatinib and erlotinib are potent reversal agents for MRP7 (ABCC10)-mediated multidrug resistance. Biochem Pharmacol. 2010 Jan 15; 79(2):154–161. [PubMed: 19720054]

41. Shen T, Kuang YH, Ashby CR, Lei Y, Chen A, Zhou Y, et al. Imatinib and nilotinib reverse multidrug resistance in cancer cells by inhibiting the efflux activity of the MRP7 (ABCC10). PLoS One. 2009; 4(10):e7520. [PubMed: 19841739]

42. Chen ZS, Hopper-Borge E, Belinsky MG, Shchaveleva I, Kotova E, Kruh GD. Characterization of the transport properties of human multidrug resistance protein 7 (MRP7, ABCC10). Mol Pharmacol. 2003 Feb; 63(2):351–358. [PubMed: 12527806]

43. Urbatsch IL, Sankaran B, Weber J, Senior AE. P-glycoprotein is stably inhibited by vanadate-induced trapping of nucleotide at a single catalytic site. J Biol Chem. 1995 Aug 18; 270(33): 19383–19390. [PubMed: 7642618]

44. Brooks TA, Minderman H, O'Loughlin KL, Pera P, Ojima I, Baer MR, et al. Taxane-based reversal agents modulate drug resistance mediated by P-glycoprotein, multidrug resistance protein, and

breast cancer resistance protein. Mol Cancer Ther. 2003 Nov; 2(11):1195–1205. [PubMed: 14617793]

45. Robbiani DF, Finch RA, Jager D, Muller WA, Sartorelli AC, Randolph GJ. The leukotriene C(4) transporter MRP1 regulates CCL19 (MIP-3beta, ELC)-dependent mobilization of dendritic cells to lymph nodes. Cell. 2000 Nov 22; 103(5):757–768. [PubMed: 11114332]
46. Sarkadi B, Homolya L, Szakacs G, Varadi A. Human multidrug resistance ABCB and ABCG transporters: participation in a chemoimmunity defense system. Physiol Rev. 2006 Oct; 86(4): 1179–1236. [PubMed: 17015488]
47. Kruh GD, Belinsky MG. The MRP family of drug efflux pumps. Oncogene. 2003 Oct 20; 22(47): 7537–7552. [PubMed: 14576857]
48. Dabrowska M, Sirotnak F. Regulation of transcription of the human MRP7 gene. Characteristics of the basal promoter and identification of tumor-derived transcripts encoding additional 5' end heterogeneity. Gene. 2004 Oct 27.341:129–139. [PubMed: 15474296]
49. Dabrowska M, Sirotnak FM. Regulation of transcription of the human MRP7 gene. Characteristics of the basal promoter and identification of tumor-derived transcripts encoding additional 5' end heterogeneity. Gene. 2004 Oct 27.341:129–139. [PubMed: 15474296]
50. Borel F, Han R, Visser A, Petry H, van Deventer SJ, Jansen PL, et al. Adenosine triphosphate-binding cassette transporter genes up-regulation in untreated hepatocellular carcinoma is mediated by cellular microRNAs. Hepatology. 2012 Mar; 55(3):821–832. [PubMed: 21932399]
51. Hlavata I, Mohelnikova-Duchonova B, Vaclavikova R, Liska V, Pitule P, Novak P, et al. The role of ABC transporters in progression and clinical outcome of colorectal cancer. Mutagenesis. 2012 Mar; 27(2):187–196. [PubMed: 22294766]

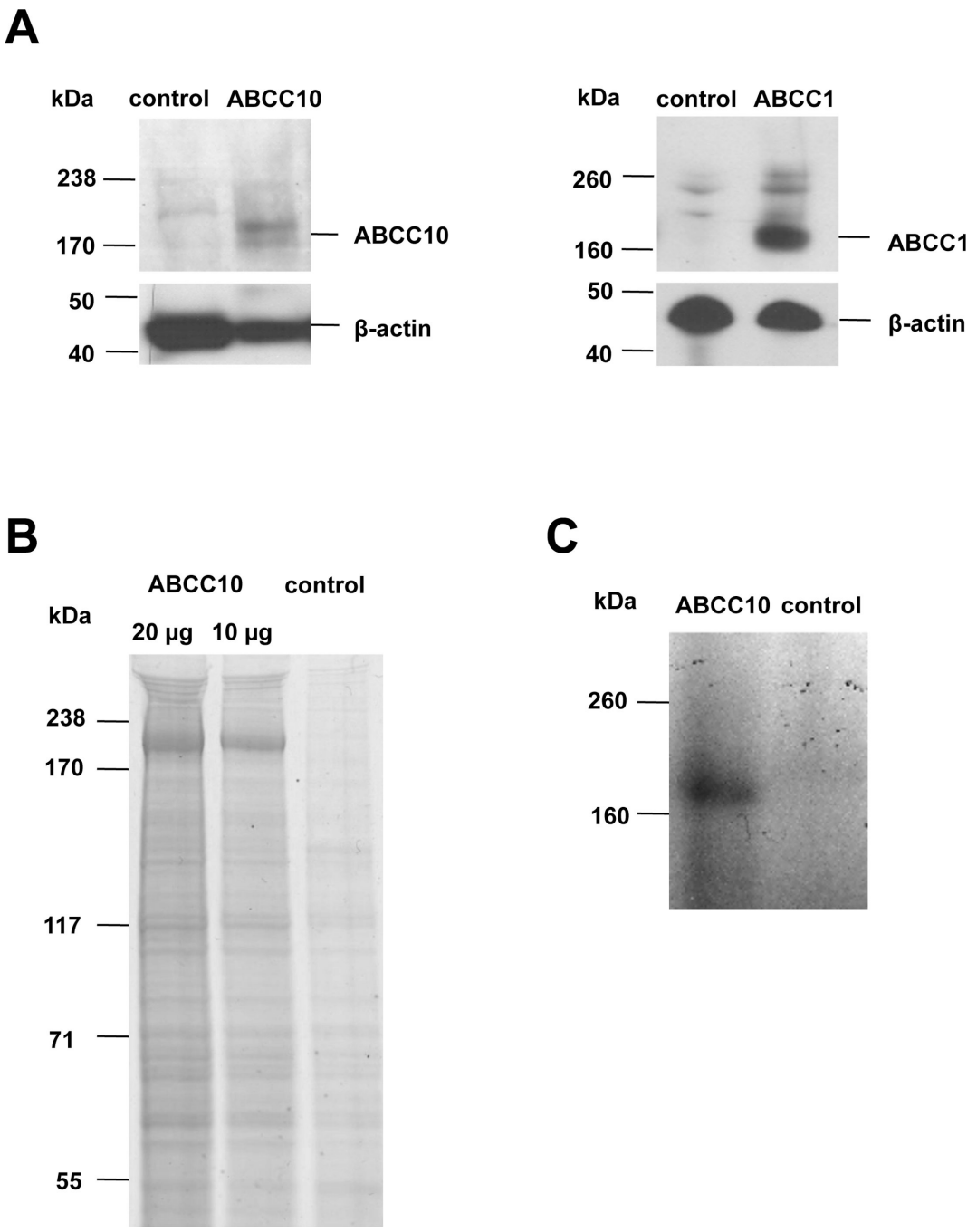

Figure 1. Detection of ABCC10 and ABCC1 in membrane vesicle preparation

A. Membrane vesicles prepared from High Five insect cells infected with ABCC10, ABCC1 or control baculovirus were resolved by SDS-PAGE and probed with anti-ABCC10 or anti-ABCC1 antibodies. Full length ABCC10 is ~191 kDa, and ABCC1 is ~170 kDa (6, 17). **B.** Colloidal blue staining of (1) 20 µg or (2) 10 µg of membrane preparation indicates no degradation. **C.** Autoradiograph indicating binding of [α-$_{32}$P]-8-azido ATP to ABCC10, after incubation of HiFive ABCC10 overexpressed membranes with [α-$_{32}$P] 8-azidoATP under a nonhydrolytic condition (4°C).

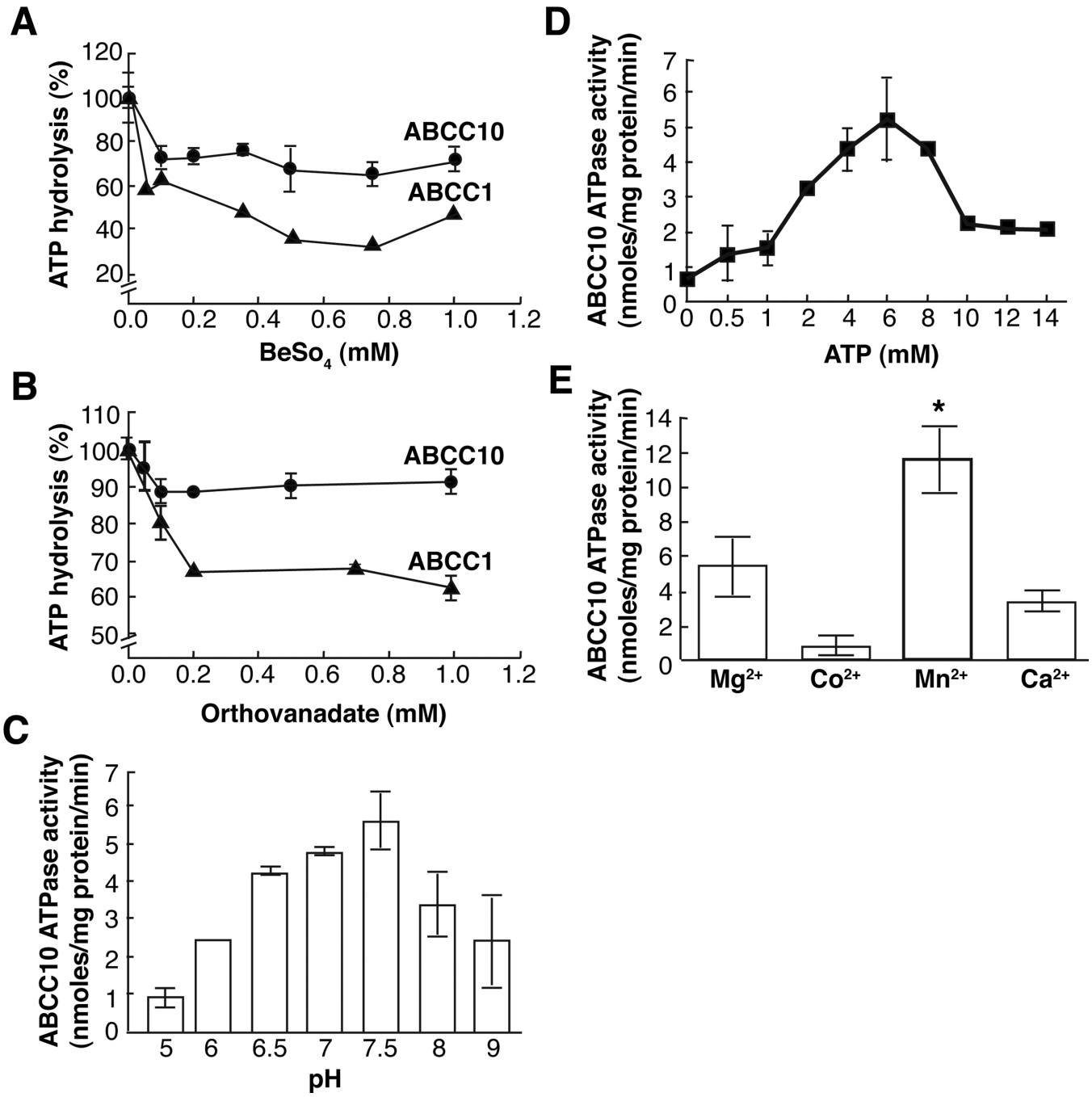

Figure 2. ABCC10 and ABCC1-mediated hydrolysis

For all experiments, data are means ± SDs of triplicate determinations. Graphs represent combined data from three separate experiments of ABCC10 (closed circles) or ABCC1, (closed triangles). **A,B.** Steady state ATP hydrolysis was measured in ABCC10 and ABCC1 containing crude membranes in the presence of increasing concentrations of BeFx (**A**) or Vi **(B). C.** ABCC10 ATPase activity at various pHs. **D.** BeFx-sensitive ABCC10 ATPase activity was measured at several ATP concentrations (2, 5, 8, 10, 12, 14 mM). **E**), ABCC10 ATPase activity of membrane protein (10 μg) was assayed with 2x assay buffer containing

10 mM $MnCl_2$, $MgCl_2$, $CaCl_2$, or $CoCl_2$. *, significant increase in ABCC10 ATPase activity (p= 0.0178) compared with Mg^{2+}.

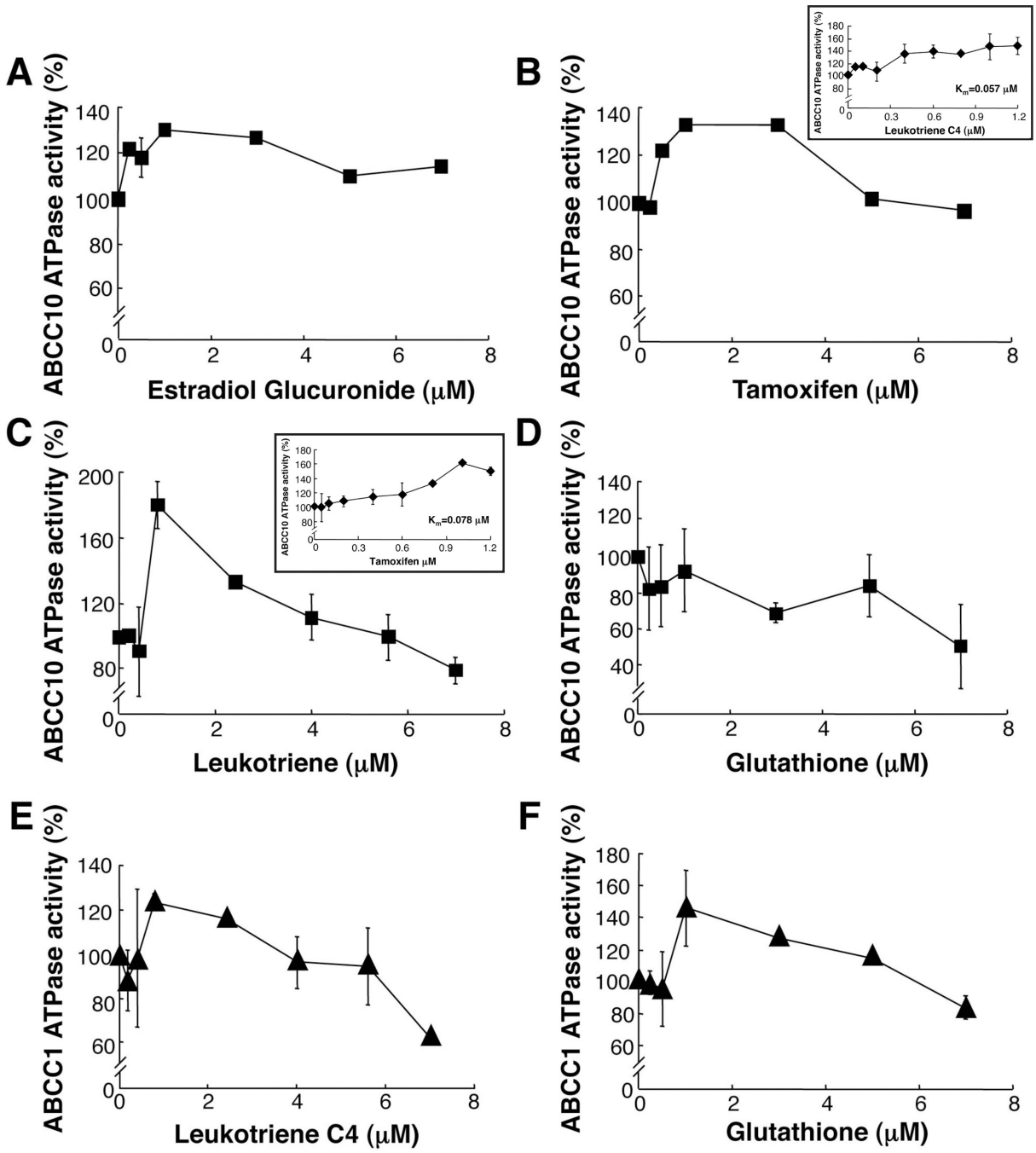

Figure 3. Effect of LTC4, GSH, E217βG and tamoxifen on ABCC10 ATPase activity

Effect of $E_2$17βG (**A**), tamoxifen (**B**), LTC_4 **(C)** or GSH **(D)** on ABCC10 ATPase activity. Effect of LTC_4 **(E)** or GSH **(F)** on ABCC1 ATPase activity. Data points are means ±SD of triplicate determination. Graphs represent combined data from three separate experiments of ABCC10 (closed circles) or ABCC1, (closed triangles).

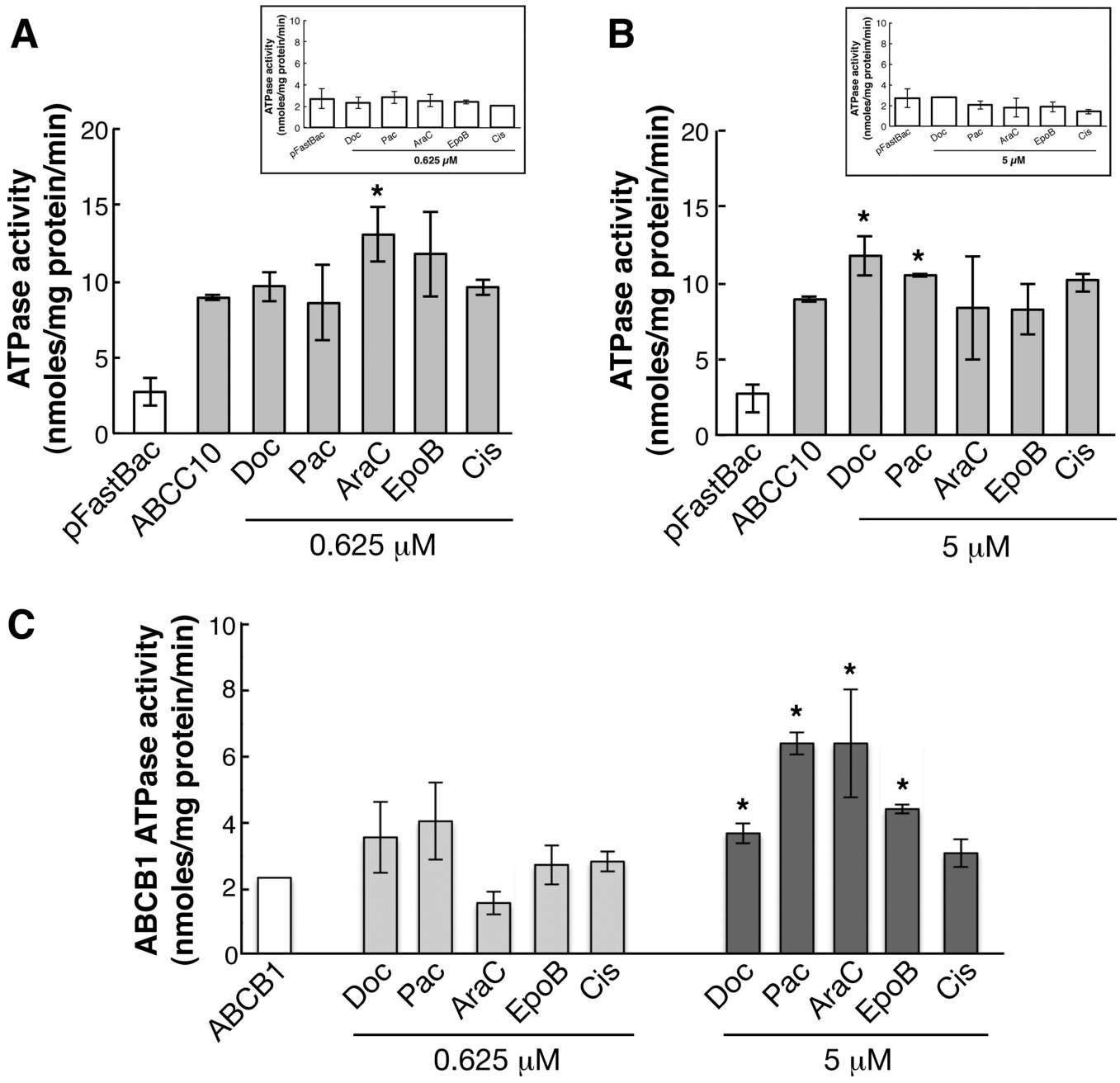

Figure 4. Stimulation of ABCC10 activity by anticancer drugs

Survey of ABCC10 (**A, B**) and pFastBac-control (**4A inset, and 4B inset**), ABCB1 (**C**) ATPase activity was performed after addition of two separate concentrations of docetaxel (Doc), paclitaxel (Pac), epothilone B (EpoB), cytarabine (Ara-C) and cisplatin (Cis). A), 0.625 μM and B), 5 μM. Bars represent the means of three separate experiments performed in duplicate ± SD. Statistical analysis was calculated using a Student's unpaired *t*-test; *P*-values for ABCC10 are 0.0288 (docetaxel), 0.0169 (paclitaxel), and 0.0124 (cytarabine); P-values for ABCB1 are 0.0456 (docetaxel), 0.0168 (paclitaxel), 0.0319 (cytarabine) and 0.0495 (epothilone B).

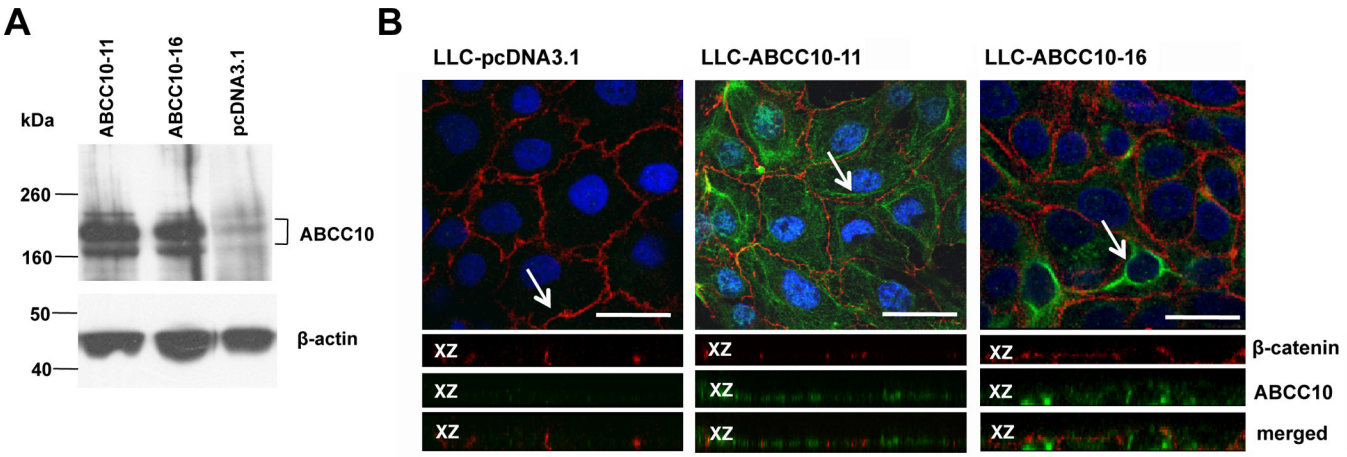

Figure 5. Detection of expression by western blot and localization of ABCC10 in LLC-ABCC10 monolayers

A. 30 μg of crude membranes prepared from LLC-PK1, LLCABCC10-11 and LLC-ABCC10-16 cells was analyzed by Western blot. The ABCC10 monoclonal antibody detected 2 bands with apparent M_r ~168,000 kDa and 202,000 kDa. **B**. Immunofluorescence analysis of confluent LLC-PK1 cells transfected with pcDNA 3.1 (left panel) and LLC-PK1 cells transfected with ABCC10 expression vector (middle panel) and (right panel). ABCC10 (green), β-catenin (red) and DAPI-stained DNA (blue) are indicated. Arrows indicate the location of xz-section shown below each panel. Scale bar, 20 μM, 60X magnification.

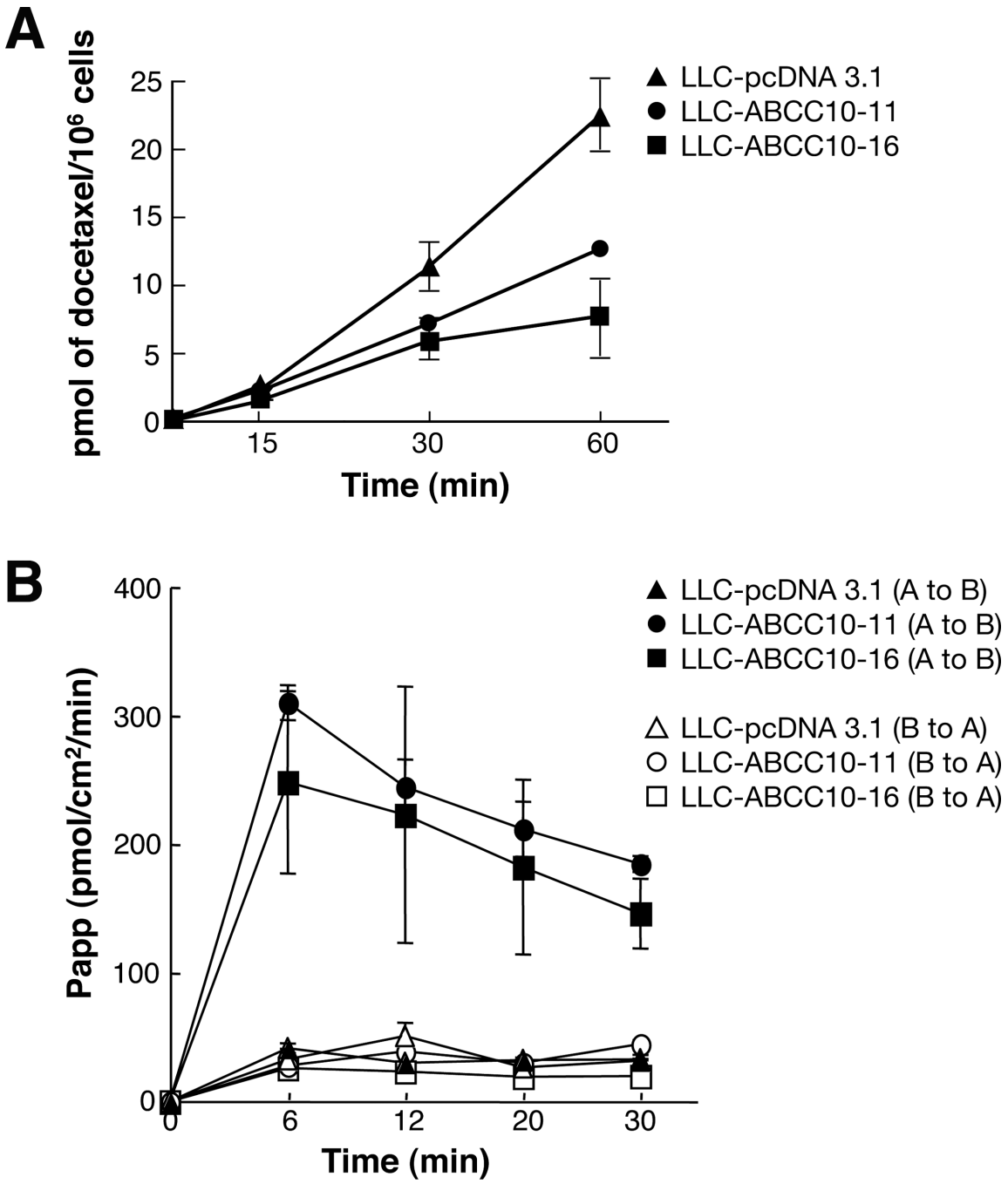

Figure 6. Accumulation and transepithelial transport of [^{3}H]-docetaxel

A. Cellular accumulation of [^{3}H]-docetaxel in LLC-PK transfected cell lines compared with parental cells. **B**. Basolateral to apical or apical to basolateral transport of [^{3}H]-docetaxel. At 6 min the *P*-values =0.0063 for LLC-ABCC10-16 and 0.0202 for LLC-ABCC10-11. Representative data is shown for LLC-ABCC10-11(circles), LLC-ABCC10-16 (squares) transfectant lines and the LLC-pcDNA3.1 control line (triangles); full symbols indicate apical to basolateral (A to B) transport and empty symbols indicate basolateral to apical (B to A) transport.

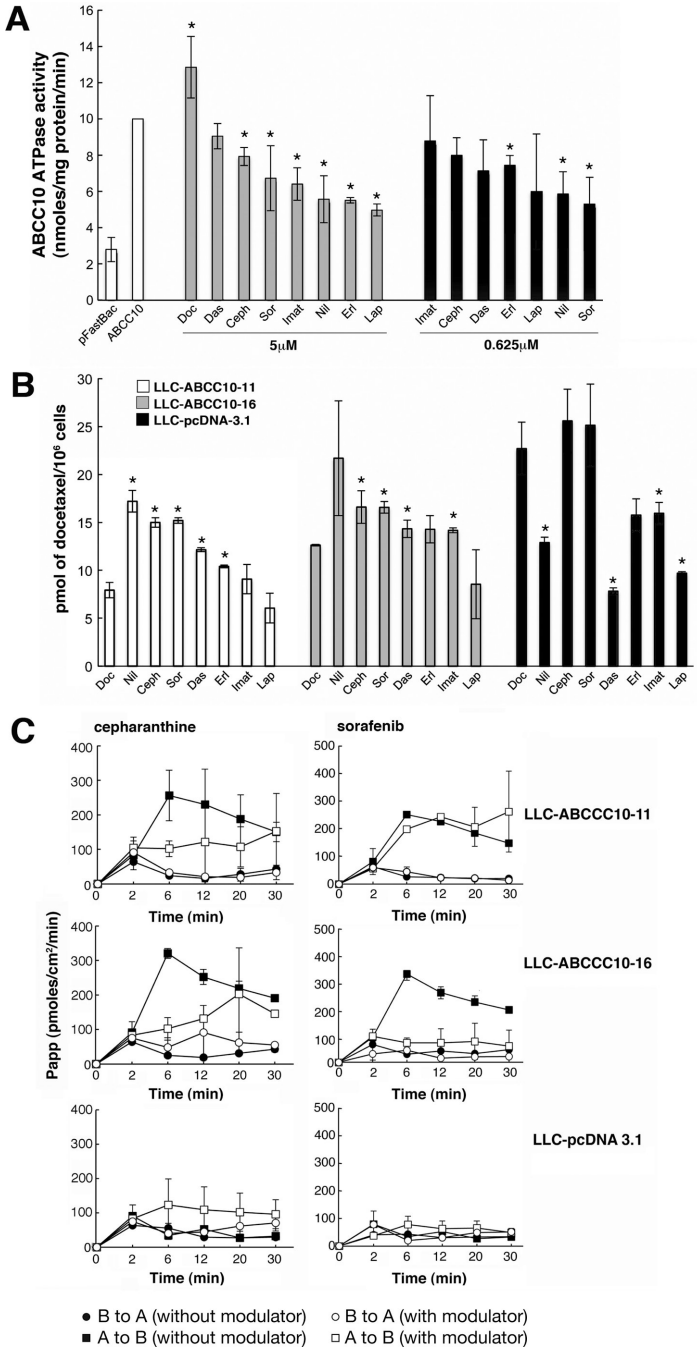

Figure 7. Effect of modulators on ABCC10 ATPase activity and accumulation of [^{3}H]-docetaxel

For all experiments, each point represents the mean ± S.D. of three experiments. **A**. ATPase activity of ABCC10 in the presence of 5μM or 0.625μM cepharanthine (Ceph) or sorafenib (Sor), dasatinib (Das), imatinib (Imat), nilotinib (Nil), erlotinib (Erl), lapatinib (Lap) [2.5μM]. *P*-values at 5 μM are 0.0219 (cepharanthine), 0.0434 (sorafenib), 0.024 (imatinib), 0.0431 (nilotinib), 0.002 (erlotinib) and 0.012 (lapatinib). *P*-values at 0.625 μM are 0.0367 (erlotinib) and 0.0333 (nilotinib) **B**. Cellular accumulation of [^{3}H]-docetaxel in cells treated with cepharanthine or TKIs. *P*-value in LLC-ABCC10-11 and LLC-ABCC16 respectively: for cepharanthine = 0.0472, 0.0218; for sorafenib = 0.0491, 0.0046; for dasatinib = 0.0155,

0.0265; for erlotinib in LLC-ABCC10-11 = 0.0423; for nilotinib in LLC-ABCC10-11 = 0.0104; for imatinib in LLC-ABCC10-16 = 0.0062. Figure 7C. Effect of modulators on the basolateral to apical or apical to basolateral transport of [^{3}H]-docetaxel. Basolateral-to-apical, and apical-to-basolateral transport of [^{3}H]-docetaxel in cells treated with cepharanthine or sorafenib. For 5μM cepharanthine treatment of LLC-ABCC10-16 and LLC-ABCC10-11, P=0.0312 and P= 0.05 at 6 min, respectively. For 2.5 μM sorafenib, the LLC-ABCC10-16 cell line showed maximal inhibition of apical to basolateral transport at 6 minutes (P= 0.0341). For all experiments, each point represents the mean ± S.D. of three experiments. Curves shown represent apical-to-basolateral transport (squares); basolateral-to-apical transport (circles); without modulator (full symbols); and with modulator (open symbols).